Defence Technology 13 (2017) 150–157

Contents lists available at ScienceDirect

Defence Technology

journal homepage: www.elsevier.com/locate/dt

An approach for optimization of the wall thickness (weight) of a thick-walled cylinder under axially non-uniform internal service pressure distribution

Onur Güngör

MKE Kurumu Mühimmat Fabrikası Ar-Ge Müdürlüğü 71100 Merkez, Kırıkkale, Turkey

ARTICLE INFO

Article history:
Received 20 January 2017
Received in revised form
2 April 2017
Accepted 20 April 2017
Available online 25 April 2017

Keywords:
Optimization
Gun tube design
Thick wall cylinder
Residual stress
Internal ballistics
Service pressure
Wall thickness
Numerical topology
Swage autofrettage
Material removal
Weight reduction

ABSTRACT

Today, improving the weight/load carrying capacity ratio of a part is the matter of studies in most of the scientific and industrial areas.

Autofrettage dimensions, the amount of material removed from outer and inner radius while manufacturing and the service pressure applied affect the residual stress distribution throughout the wall thickness and hence the load-bearing capacity of a thick-walled cylinder. Calculation of residual stresses after autofrettage process and optimization of autofrettage outline dimensions by using the amount of service pressures applied are common issues in literature.

In this study, mandrel-cylinder tube interference dimensions were renovated by using traditional methods for swage autofrettage process of a gun barrel. Also, the residual stresses in the cylinder after autofrettage process, inside and outside material removal process and the variable service pressure throughout the cylinder applied were taken into consideration and incorporated into the design. By using the constrained optimization method, wall thickness (thus the weight) was optimized (minimized) to achieve the specified safety factor along the length of the cylinder. For the same cylinder, the results of the suggested analytical/with residual stress calculation approach were compared to analytical/without residual stress calculation results and numerical topology optimization method calculation results. Since the experimental measurement results are not yet available, it was not possible to compare them with the calculation results.

The suggested approach enabled 22.9% extra weight reduction in proportion to numerical topology optimization and enabled 4.2% extra weight reduction in proportion to analytical/without residual stress optimization.

Using this approach, the gain from residual stresses after autofrettage operation, the loss of residual stresses after material removal, and the effects of service pressures can be taken into account for each stage of design.

1. Introduction

Different amount of service pressures is applied on thick wall cylinders in accordance with the applications they used for. In order cylindrical tube to do its duty safely, internal pressure should not cause plastic deformation while using the cylinder. For making proper pressurized vessel/tube design, one should need to know the residual stress distribution of the autofrettaged cylinder while applying the service pressure. Optimization of autofrettage relies on the stress distribution which is the result of the service pressure to be applied.

After autofrettage process, an amount of material is often removed from inner and/or outer surfaces of the pressurized vessel/tube. Material removal process for heavy arm gun barrel is performed both to inner and outer surfaces to manufacture the conjunctions, to shape the outer surface of the barrel, to open the groove sets and to shape the chamber. These are the material removal and hence the weight loss possibilities of a gun barrel but it also changes the residual stress distribution along every single millimeters of the length and the radius. In this study, optimized autofrettage and subsequent residual stresses, internal and external

E-mail address: onur.gungor@mkek.gov.tr.
Peer review under responsibility of China Ordnance Society.

http://dx.doi.org/10.1016/j.dt.2017.04.003

material removal and distributing service pressure along the length of the barrel were taken into consideration to optimize the wall thickness (weight) of the barrel.

Davidson et al. [1] compared the results of the experiments they had performed with the theoretical results to see how the residual stresses in the mechanical autofrettage process change depending on the extreme strain and diameter ratio. Jost [2] elaborated analytically the stresses and strains that occurred during the reaming process applied by a mandrel passing through a cylinder. Jahed et al. [3] used a simple back and forth torsion test to determine the unloading behavior of the NiCrMoV12.5 steel and found that the material exhibits excellent plastic behavior during loading and nonlinear behavior during reverse loading. Parker et al. [4] summarized different models for evaluating the effect of material removal on residual stresses. They incorporated the Bauschinger effect into an analytical method for estimating residual stresses in the autofrettage process for an elastic-perfect plastic model. Ayob et al. [6], investigated autofrettaged thick wall cylinders for stress distributions at working pressures and it has been determined that the maximum equivalent stress in the working pressure occurs at the plastic-elastic transition radius of the cylinder. Ali et al. [7], using the finite element method, investigated how the factors such as the ratio of outside diameter to inside diameter of a cylindrical tube, working pressure, material model and autofrettage level affect the utility obtained from autofrettage process. Johnsen [8] implemented structural topology optimization technique for recycled aluminum material for a plane control door. Hu et al. [9] simulated the mechanical autofrettage process for a heavy arm gun barrel with a finite element program. Yıldırım [10] investigated swage autofrettage process for a heavy arm gun barrel.

2. Material and methods

Assumptions and steps;

Distributing service pressure was applied only the inner wall of the cylinder.
This was an open-end, thick walled cylinder (axial stress is accepted constant and close to zero).
The sum of the plastic strain components was equal to zero.
The value of shear stress at the mandrel-tube frictional surface was neglected because it was very small alongside the other stress components.
Mandrel exhibited elastic behavior at every moment of the autofrettage process.
The elastic-linear plastic material model was used for the cylinder.
The effect of residual stress values from autofrettage and material removal was not able to be included in the numerical topology optimization calculation.
First, autofrettage optimization was carried out and plastic-elastic transition diameter was determined. Internal diameter expansion (loading) was applied, permanent stresses were calculated after discharging the load (unloading) and no secondary-flow occurred in the cylinder inner wall after load discharge (unloading).
Optimum autofrettage dimensioning of the draft tube was then carried out for the highest service load value (400 MPa) and autofrettage residual stresses were calculated.
Material removed from the inner radius was assumed to be constant in thickness along the barrel. The outer radius was considered to be suitable for variable material removal, and the state of residual stresses after material removal was calculated.

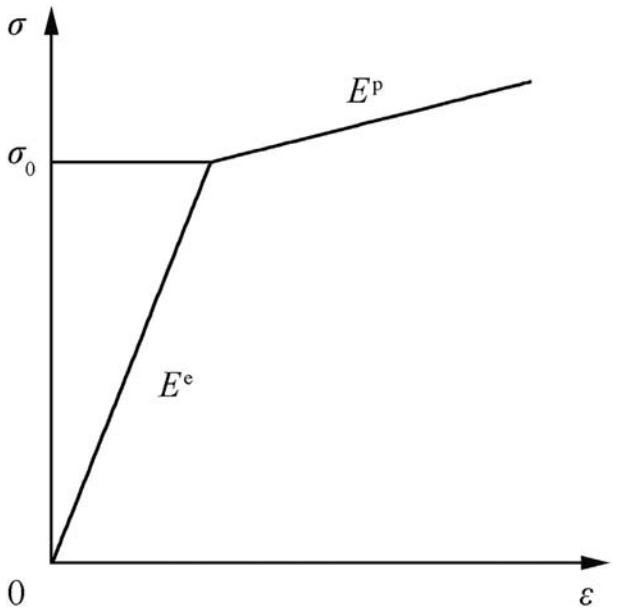

Fig. 1. Elastic-linear plastic material model.

Material removal was calculated for each millimeter of the gun barrel by using three different optimization approach and resulting optimized thicknesses were compared to each other. In the analytical thickness optimization, different levels of the safety factor of the material were used. In the numerical topology optimization, the value of the cylinder yield stress, at which, the safety factor equals 1.0, was used as the constraint value. So, Von Mises equivalent stress values were calculated and the comparison of different approaches was made for the case at which the safety factor was 1.0.

2.1. Material model

2.1.1. Elastic-linear plastic model

Elastic-linear plastic model is a more real like stress-strain model when it is compared to the elastic-perfectly plastic model (See Fig. 1). The stress-strain relation for the elastic-linear plastic model can be expressed as follows

$$\varepsilon = \frac{\sigma}{E^e} \quad (\sigma < \sigma_0) \tag{1}$$

$$\varepsilon = \frac{\sigma}{E^e} + \frac{1}{E^p}(\sigma - \sigma_0) \quad (\sigma > \sigma_0) \tag{2}$$

For use in analytical and numerical calculation, the data obtained by analyzing the result of uniaxial tensile test of the materials are shown below (See Table 1). The mandrel material is tungsten.

Table 1
Material properties.

Property	Gun barrel material	Tungsten
E^e/GPa	141	450
υ	0.29	0.28
σ_0/MPa	1086.01	–
E^p/GPa	2.36	–

2.2. Analytical approach

2.2.1. Determination of the elastic-plastic junction

The interference which is represented by the symbol I is defined by the difference between the outer radius of the mandrel and the inner radius of the cylinder.

$$I = r_m - a \tag{3}$$

Mandrel that is used for the swage autofrettage process is manufactured from a material having high elastic modulus. Therefore, the cylindrical tube is subject to plastic deformation but only the elastic deformation is observed on the mandrel.

The pressure to the mandrel in the calculation of the autofrettage pressure is the negative sign of the radial tension occurring at radius a during the shape change of the tube where$r = a$. By using the above assumptions and organizing the formulas for the elastic and plastic region, one can find the autofrettage pressure and the interference formulas

$$\dot{P} = \frac{\frac{\sigma_0}{2}\left[1 - \frac{c^2}{b^2} + \ln\frac{c^2}{a^2} + (1-\nu^2)\frac{E^p}{E^e}\left(\frac{c^2}{a^2} - \frac{c^2}{b^2}\right)\right]}{1 + (1-\nu^2)\frac{E^p}{E^e}} \tag{4}$$

$$I = (1-\nu)\frac{\sigma_0 c^2}{2Ga} - a(1-2\nu)\frac{\dot{P}}{2G} - \frac{\dot{P}}{E_m}a(2\nu_m - 1)(\nu_m + 1) \tag{5}$$

To find$c$, an iteration should be applied to the equation. The radius of intersection c is the most important parameter of analytical wall thickness optimization. The left side of the equation is unchanged (mandrel and cylinder radii in the first case), on the right side a is changed in a certain range and c is precisely changed from a to b, when the right and left sides of the equation are equal to each other less than 0.0001, the value of c found is the plastic-elastic transition radius (See Fig. 2). Thus, according to the characteristics of the mandrel and the cylinder, the amount of expansion and contraction is distributed to the mandrel and the cylinder.

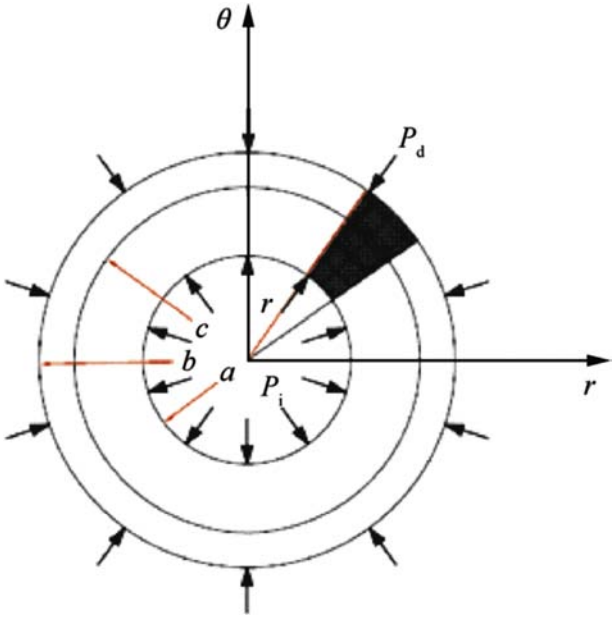

Fig. 2. Common loading and radii representation of a thick wall cylinder.

2.2.2. Residual stresses after mandrel force unloading

Residual Stresses in the Plastic Region $(c - b)$

$$\sigma_r^R = \frac{-\frac{\sigma_0}{2}\left[1 - \frac{c^2}{b^2} + \ln\frac{c^2}{r^2} + (1-\nu^2)\frac{E_t}{E}\left(\frac{c^2}{r^2} - \frac{c^2}{b^2}\right)\right]}{1 + (1-\nu^2)\frac{E_t}{E}} - \left(\frac{\dot{P}a^2}{b^2 - a^2}\right)\left(1 - \frac{b^2}{r^2}\right) \tag{6}$$

$$\sigma_\theta^R = \frac{\frac{\sigma_0}{2}\left[1 + \frac{c^2}{b^2} - \ln\frac{c^2}{r^2} + (1-\nu^2)\frac{E_t}{E}\left(\frac{c^2}{r^2} + \frac{c^2}{b^2}\right)\right]}{1 + (1-\nu^2)\frac{E_t}{E}} - \left(\frac{\dot{P}a^2}{b^2 - a^2}\right)\left(1 + \frac{b^2}{r^2}\right) \tag{7}$$

Residual Stresses in the Elastic Region $(a - c)$

$$\sigma_r^R = \frac{\sigma_0}{2}\left(-\frac{c^2}{r^2} + \frac{c^2}{b^2}\right) - \left(\frac{\dot{P}a^2}{b^2 - a^2}\right)\left(1 - \frac{b^2}{r^2}\right) \tag{8}$$

$$\sigma_\theta^R = \frac{\sigma_0}{2}\left(\frac{c^2}{r^2} + \frac{c^2}{b^2}\right) - \left(\frac{\dot{P}a^2}{b^2 - a^2}\right)\left(1 + \frac{b^2}{r^2}\right) \tag{9}$$

2.2.3. Determination of the effects of material removal after autofrettage on residual stresses

In this section, the effect of material removal from the internal or external surface on permanent stresses will be analytically addressed.

If we consider the negative expression of the permanent radial stress in the inner radius a′ and the outer radius b′ as the hydrostatic pressure applied from $r = a$ or b, we can express the pressure change occurring on these surfaces after turning.

$$\dddot{\Delta} P = P_{a'_2} - P_{a'_1} \tag{10}$$

$$\dddot{\Delta} P = P_{b'_2} - P_{b'_1} \tag{11}$$

The new internal radii after turning (a'_2 and b'_2) equals zero. The elastic stresses produced by the pressure change $\dddot{\Delta} P$ can be expressed as follows for inside and outside material removal respectively. As will be noted, the inner radius grows and the outer radius shrinks.

$$\sigma_r = \left(\frac{\dddot{\Delta} Pa'^2}{b^2 - a'^2}\right)\left(1 - \frac{b^2}{r^2}\right) \tag{12}$$

$$\sigma_\theta = \left(\frac{\dddot{\Delta} Pa'^2}{b^2 - a'^2}\right)\left(1 + \frac{b^2}{r^2}\right) \tag{13}$$

$$\sigma_r = \left(\frac{-\Delta^{\cdots} Pb'^2}{b'^2 - a^2}\right)\left(1 - \frac{a^2}{r^2}\right) \tag{14}$$

$$\sigma_\theta = \left(\frac{-\Delta^{\cdots} Pb'^2}{b'^2 - a^2}\right)\left(1 + \frac{a^2}{r^2}\right) \tag{15}$$

The new stress distribution are obtained by superposition of the elastic stresses produced by the pressure difference $\dddot{\Delta} P$ caused by the material removal and the autofrettage residual stresses.

2.2.4. Determining the stresses occurring in autofrettaged cylinders at service pressure

The stresses in the thick walled cylinders that are subject to operating pressure are obtained by the superposition of the elastic stresses that are produced by the service pressure and residual stresses that are produced by autofrettage and material removal processes.

$$\sigma_{\text{total}} = \sigma_{\text{ser}} + \sigma^{\text{R}} \tag{16}$$

$$(\sigma_{\text{r}})_{\text{ser}} = \left(\frac{\text{P}_{\text{ser}}a^2}{b^2 - a^2}\right)\left(1 - \frac{b^2}{r^2}\right) \tag{17}$$

$$(\sigma)_{\theta\text{ser}} = \left(\frac{P_{\text{ser}}a^2}{b^2 - a^2}\right)\left(1 + \frac{b^2}{r^2}\right) \tag{18}$$

2.3. Implementation and comparison of analytical weight optimization and numerical topology optimization methods to reduce barrel weight

2.3.1. Projectile movement in the barrel

The projectile starts to move (x_0) and accelerate with the effect of the gunpowder gas expanding with the gunpowder firing in the barrel. The highest service pressure value affecting the gun barrel and projectile is $P_{\text{s max}}$. However, when designing, the highest pressure value is taken into account in all of the points along which the service pressure will be effective prior to the highest service pressure position (x_{max}). Moreover, this value is higher than the service pressure ($P_{B\ \text{max}}$). When the projectile moves in the barrel, the pressure value falls parabolic after the point at which the highest pressure occurs, and takes the lowest value at the end of the barrel. In general, all combustion events in the barrel occur in the following manner (See Fig. 3).

In the following sections, barrel wall thickness optimization was first considered analytically and autofrettage mentioned in the previous headings, machining after autofrettage, and finally the application of service pressures was calculated and wall thicknesses were determined. Then, the wall thickness change was determined by numerical topology optimization technique, compared to others and evaluated.

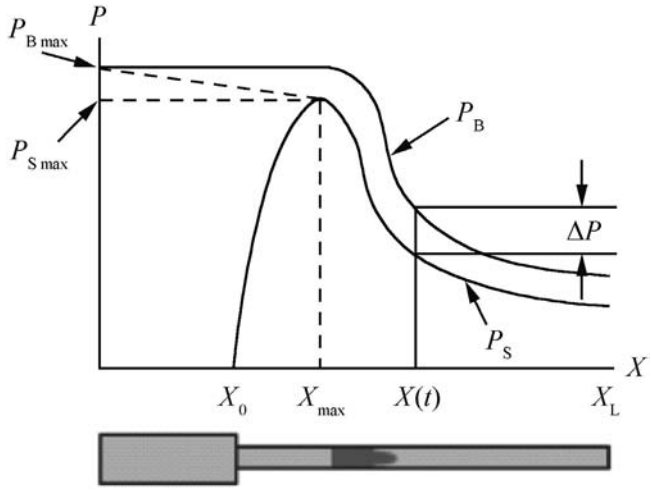

Fig. 3. Typical barrel internal ballistic. Pressure-distance graph [5].

2.3.2. Analytical thickness (weight) optimization

The safety calculation for each millimeter cross-section along the barrel was made with computer code to optimize its wall thickness (weight). First, the residual stresses are calculated after autofrettage, and the calculation is made so that the internal diameter enlargement amount is applied constantly during the material removal account and the maximum reduction is achieved by continuously changing (reducing) the external diameter in accordance with the safety factor for each millimeter of the length of the barrel. The equivalent stress values were calculated for the case of applying the design pressure (See Fig. 4-Red curve) and for the elastic-plastic transition radius at which all equivalent stress values are highest.

In this way, the advantage obtained by residual stress could be evaluated by using Von Mises Flow Criterion and superposing the critical stress state formed by the loss caused by the material removal process and as a result of applied design pressure.

The parameters that could not be evaluated are the torque that the barrel induced by the projectile twist on the grooves-sets and the decrease the strength of the steel which may be caused by heating of the barrel for repeating fires.

2.3.3. Numerical topology (geometry) optimization

By the development of computers and commercial softwares over the past decade, computer-aided design, engineering and production have been widely used by commercial firms and researchers. The increasing use of computation power and the optimization algorithms are increasingly being used to design products efficient and robust.

The topology optimization is to organize the new construction by reducing elements within and outside the construction, taking into account that the structural elements consisting of the lattice elements are appropriate to the load carrying profile formed within the loading conditions and constraints, but carrying the loads in similar robustness to the base design. In doing so, the topology to be applied is determined by considering the weight/performance ratio of the graded parts and the time to be earned.

In topology optimization, according to the state of transportation of the load, both internal and external element reduction is applied. For gun barrel, it was deemed to be more appropriate not to allow material depletion from inside. In this way, topology

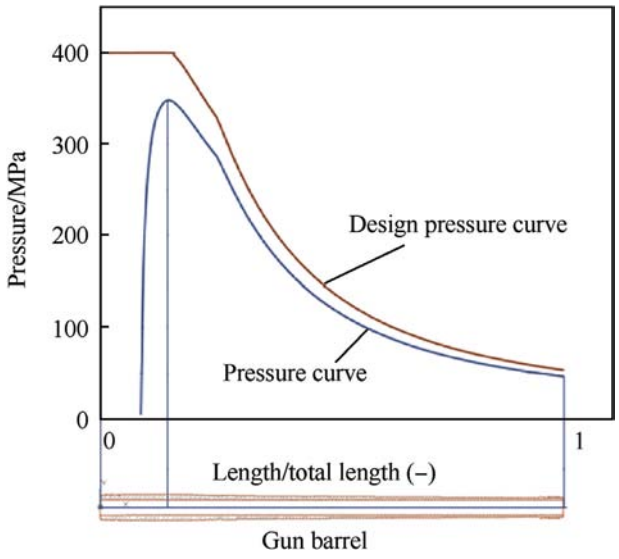

Fig. 4. Internal ballistic pressure distribution curves and corresponding points on the barrel.

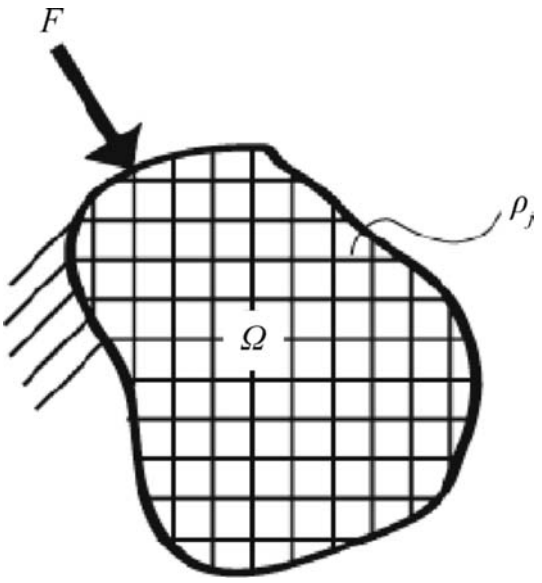

Fig. 5. Abstract model of design space showing load and boundary conditions [8].

optimization was used in form and dimensional optimization.

In Finite Elements Method, the topology optimization can be expressed as follows.

The elements describe the geometry, density and elastic modulus describe the material (See Fig. 5). The load density on the elements according to the boundary and loading conditions takes a value of 0–1 for that element in the optimization cycle. Elements having load density close to zero or less than the evaluation grade determined by the user, can be emptied from the geometry as erasable elements. In this way, the emptied volume specifies the amount of reduced weight. Elements close to one represent elements that must remain on the geometry since they are elements that actively carry the load.

2.3.3.1. Finite elements method topology optimization model. Abaqus Tosca optimization Module [11] were used for the numerical calculation of barrel weight optimization. The Condition-Based Optimization method was selected. Design reactions were

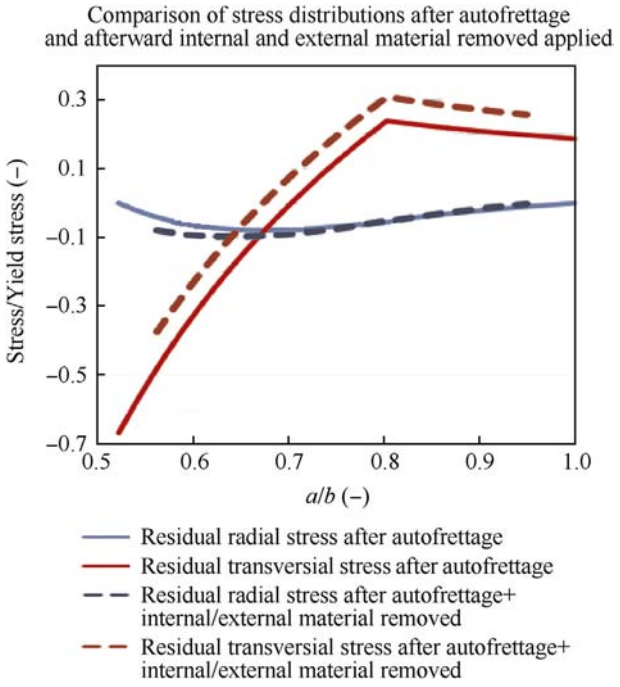

Fig. 7. Comparison of residual stresses after autofrettage and stresses in the case of internal and external material removal after autofrettage.

determined as strain energy and volume. The solver performed a number of calculations to determine user-specified gain in volume to keep the stiffness at the maximum level while reducing strain energy to the minimum and checked whether the target had been reached.

Materials were not allowed to be deleted from the planes symmetry boundary conditions applied and the regions loads applied.

Similar to the analytical calculation, the pressure changing throughout the length of the barrel was applied by defining an analytical plane at which pressure-distance curve applied to the inner wall of the barrel (See Fig. 6). The inner diameter of the

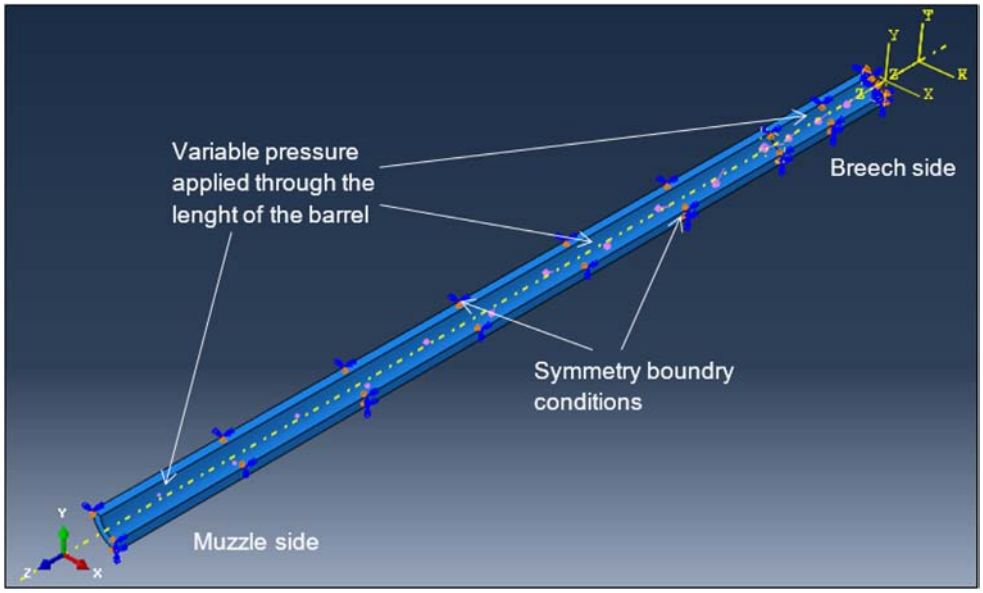

Fig. 6. Topology Optimization model boundary and loading conditions.

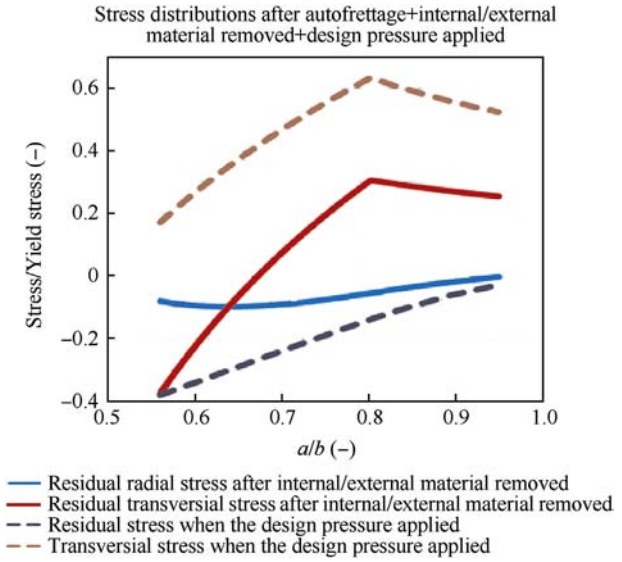

Fig. 8. Stress distribution for autofrettaged + material removed and service pressure applied.

cylinder at which constant amount of material was removed from the inner wall after autofrettage application was the inner diameter of the cylinder at the beginning of the optimization calculation.

3. Results and discussion

3.1. Stress distribution in cylinder after autofrettage and material removal processes

The following result was obtained when an amount of material was removed from the inner and the outer diameter after the autofrettage process were compared with residual stress distribution right after autofrettage (for an individual design point along the length of the barrel) (See Fig. 7).

3.2. Stress distributions of material removal after the autofrettage process and after service pressure applied inside the cylinder

After autofrettage, the following results were obtained and compared when the internal and external materials were removed and afterward when the 400 MPa service pressure was applied which the stress distribution was determined by applying superposition (See Fig. 8).

To compare, all calculations were done by using safety coefficient of 1.0. Compared to the analytically optimized barrel dimensions with the safety factor of 1.0, and the barrel dimensions obtained with the topology optimization and analytical calculation without the effect of residual stresses, the weight that could be achieved by analytical calculation with residual stresses was found to be lighter than the weight obtained by others. The reason for this was that the positive effects of autofrettage residual stresses and the negative effects of material removal could be incorporated into the analytical optimization with residual stress calculations.

The topology optimization calculation was carried out in 15 steps. The geometry acquired after the calculation is given below. The most compelling part is the chamber which the wall thickness is thicker, as the barrel comes to the end, the wall thickness decreases with decreasing pressure effect. The stress values at the chamber were tumbled to the yield strength value (1089 MPa) by the solver (See Fig. 9 and Fig. 10).

In the first calculation of the topology optimization, the residual stresses obtained from autofrettage were included but, as a result of the calculation, material depletion condition occurred abnormal along the radius of the barrel wall according to the equivalent stress distribution of the barrel (See Fig. 11). Topology optimization calculation tried to empty almost in the middle of wall thickness where equivalent stress minimum but material removal not applicable. So that, autofrettage effects were excluded from topology calculation because of impossible production of the barrel in this way.

When we look at the form obtained by topology optimization, we can see that this calculation allows the removal of more material compared to analytical/without residual stress calculations on the chamber side of the barrel, but it does not allow the decrease

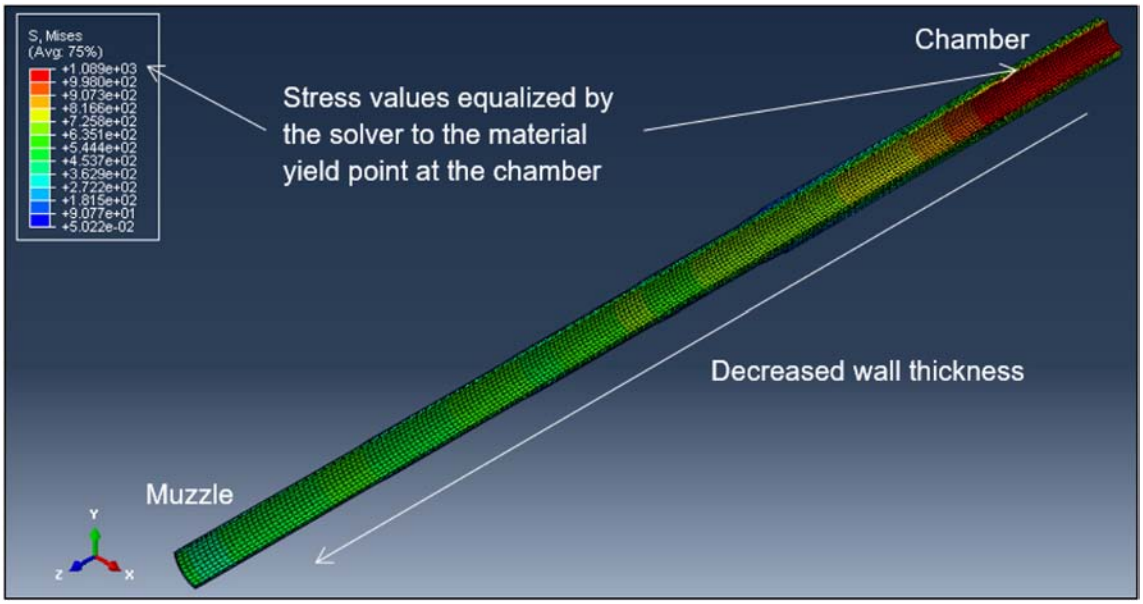

Fig. 9. The weight optimized quarter symmetrical model.

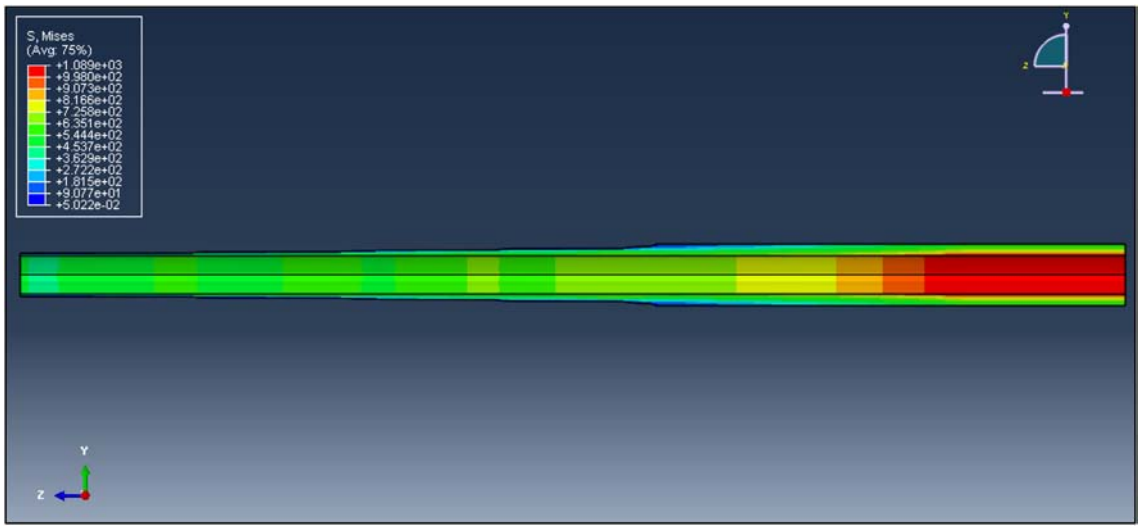

Fig. 10. The weight optimized half symmetrical model.

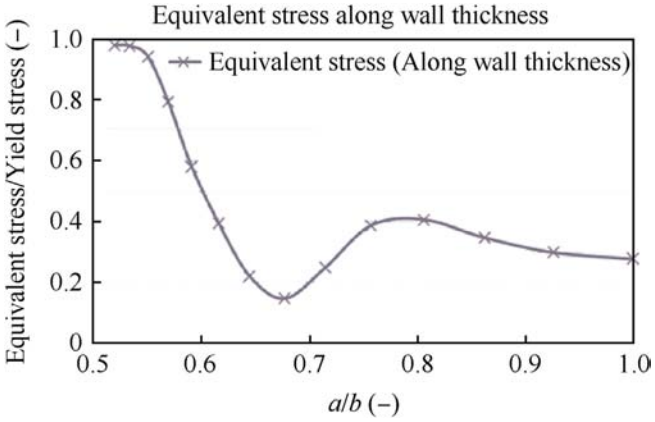

Fig. 11. Equivalent stress change along wall thickness.

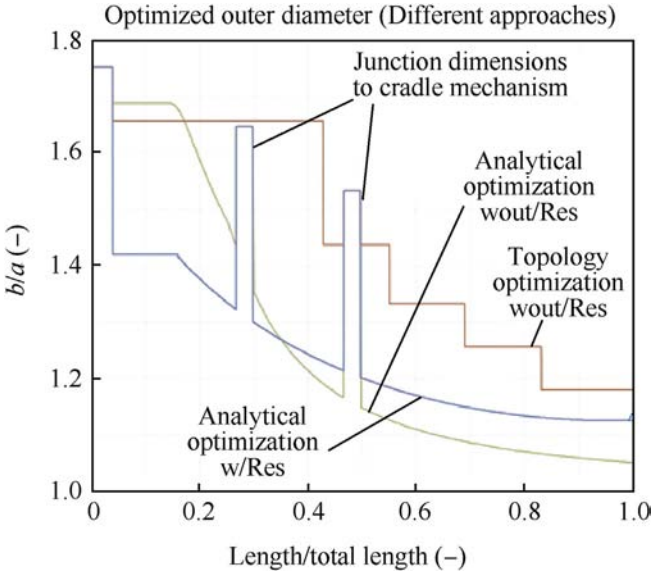

Fig. 12. Comparison of analytically optimized and topology optimized models with a safety coefficient of 1.0.

of the barrel wall thickness even though the pressure falls rapidly far before the middle of the barrel. Right before the middle and to the end of the barrel, step by step increase of material removal can be seen (See Fig. 12).

General observation, it can be said that in the analytical/without residual stress calculation, calculated wall thinning is relevant to the pressure profile and which is similar to the form obtained by the analytical/with residual calculation. However, in detail, it was determined that in the first 35% of the length of the barrel, the analytical/with residual stress calculation enables more aggressive removal of material compared to analytical/without residual stress calculation. After this section, analytical/without residual stress calculation enables the removal of more material than the analytical/with residual stress calculation but causing no significant differences. The factor that is effective here is the loss in residual stresses due to the removal of material in the analytical/with residual stress calculation. As the amount of the removed materials increase, the analytical/with residual stress calculation is interpreted as being more conservative on material removal than the analytical/without residual stress calculation. In this case, however, suggested analytical/with residual stress calculation method enables to incorporate positive and negative effects of residual stresses in the high/low-pressure zones, so that more materials can be removed in total compared to analytical/without residual stress and numerical topology optimization calculations.

Since the experimental measurement results are not yet available, it was not possible to compare them with the calculation results.

Compared to the first mass of the cylinder tube which internal and external diameters are constant throughout the length; It can be possible to remove material; 47.8% by using topology without residual stress optimization, 66.5% by using analytical/without residual stress optimization and 70.7% by using suggested analytical/with residual stress optimization.

The proposed approach in which all production and service phases are taken into account for optimization of weight can be utilized at decision phases to change the dimensions and decrease the weight of very beginning draft cylinder.

In the future study, the optimized dimensions determined by using the proposed approach will be verified using a residual stress calculation model that is constructed in accordance with the gun barrel inner ballistics including the pressure following the movement of the projectile by the help of the numerical method. In

another study, it will be demonstrated the consistency of the optimization calculations and the measurement data obtained by performing shot tests on the heavy gun barrel to be produced using the optimized dimensions.

Acknowledge

The author would like to thank Ministry of Science, Industry, and Technology which supported the project under the Industrial Thesis Support Program, to Ankara Yıldırım Beyazıd University and MKE Corporation and to everyone who contributed to the Project.

Nomenclature

Symbol	Meaning
a	Inner radius of the cylinder
b	Outer radius of the cylinder
$a/borb/a$	Diameter ratio
c	Elastic-plastic radius
E^{e}	Modulus of elasticity
E^{p}	Tangent modulus
G	Shear modulus of cylinder
I	Interference
$\dot{P}$	Autofrettage pressure
$\dot{\Delta} P$	Pressure difference because of material removal
P_{i}	Inner pressure
P_{d}	Outer pressure
P_{ser}	Service pressure
$P_{s\ max}$	Maximum pressure inside the gun barrel
$P_{B\ max}$	Design pressure of gun barrel
$P_{a'_2}$	Pressure of inner diameter after material removal
$P_{b'_2}$	Pressure of outer diameter after material removal
$P_{a'_1}$	Pressure of inner diameter before material removal
$P_{b'_1}$	Pressure of outer diameter before material removal
r	Radius
r_{m}	Outer radius of the mandrel
σ_{r}	Radial stress
σ_{θ}	Tangential stress
σ_{z}	Axial stress
σ_{0}	Yielding stress
σ_{ser}	Service stress
σ_{total}	Total stress
σ^{R}	Residual stress
σ_{r}^{R}	Radial residual stress
σ_{θ}^{R}	Tangential residual stress
ν	Poisson's ratio of cylinder
ν_{m}	Poisson's ratio of mandrel
x_{0}	Projectile movement starting point
x_{max}	Maximum pressure point inside the gun barrel

References

[1] Davidson TE, Kendall DP, Reiner AN. Residual stresses in thick-walled cylinders resulting from mechanically induced overstrain. Exp Mech 1963:253–68.
[2] Jost GS. Stresses and strains in a cold-worked annulus, Aircraft Structures. Report 434. Melbourne, Australia: Defense Science and Technology Organization, Aeronautical Research Laboratory; 1988.
[3] Jahed H. A variable material approach for elastic-plastic analysis of proportional and nonproportional loading. Thesis (PhD). University of Waterloo; 1997.
[4] Parker AP, Underwood JH, Kendall DP. Bauschinger effect design procedure for autofrettaged tubes including material removal and sachs' method. ASME J Press Vessel Technol 1999;121:430–7.
[5] Carlucci DE, Jacobson SS. Tube design, ballistics theory and design of guns and ammunition. 1st ed. New York: CRC Press; 2007. p. 163–73.
[6] Ayob A, Elbasheer MK. Optimum autofrettage pressure in thick cylinders. J Mek 2007;24:1–14.
[7] Ali ARM, Ghosh NC, Alam TE. Optimum design of pressure vessel subjected to autofrettage process. Int Sch Sci Res Innov 2010;4(10):582–7.
[8] Johnsen S. Structural topology optimization. Basic theory, methods and applications. Master Thesis. Norwegian University of Science and Technology; 2013.
[9] Hu Z, Penumarthy C. Computer modeling and optimization of swage autofrettage process of a thick-walled cylinder incorporating bauschinger effect. Am Trans Eng Appl Sci 2014;3:31–63.
[10] Yıldırım H. Analytical and numerical analysis of swage autofrettage process applied to thick walled cylinders. Master Thesis. Yıldırım Beyazıt Üniversitesi; 2015.
[11] Abaqus User's Manual, Abaqus Release 6.13 Documentation, Abaqus Inc.